

# Disruption of crosstalk between the fatty acid synthesis and proteasome pathways enhances unfolded protein response signaling and cell death

Joy L. Little,<sup>1</sup> Frances B. Wheeler,<sup>1</sup>  
Constantinos Koumenis,<sup>2</sup> and Steven J. Kridel<sup>1</sup>

<sup>1</sup>Department of Cancer Biology, Comprehensive Cancer Center, Wake Forest University School of Medicine, Winston-Salem, North Carolina and <sup>2</sup>Department of Radiation Oncology, University of Pennsylvania School of Medicine, Philadelphia, Pennsylvania

## Abstract

Fatty acid synthase (FASN) is the terminal enzyme responsible for fatty acid synthesis and is up-regulated in tumors of various origins to facilitate their growth and progression. Because of several reports linking the FASN and proteasome pathways, we asked whether FASN inhibitors could combine with bortezomib, the Food and Drug Administration-approved proteasome inhibitor, to amplify cell death. Indeed, bortezomib treatment augmented suboptimal FASN inhibitor concentrations to reduce clonogenic survival, which was paralleled by an increase in apoptotic markers. Interestingly, FASN inhibitors induced accumulation of ubiquitinated proteins and enhanced the effects of bortezomib treatment. In turn, bortezomib increased fatty acid synthesis, suggesting crosstalk between the pathways. We hypothesized that cell death resulting from crosstalk perturbation was mediated by increased unfolded protein response (UPR) signaling. Indeed, disruption of crosstalk activated and saturated the adaptation arm of UPR signaling, including eIF2 $\alpha$  phosphorylation, activating transcription factor 4 expression, and X-box-binding protein 1 splicing. Furthermore, although single agents did not activate the alarm phase of the UPR, crosstalk interruption resulted in activated c-Jun NH<sub>2</sub>-terminal kinase and C/EBP homologous protein-dependent cell death. Combined, the data support the concept that the UPR balance between

adaptive to stress signaling can be exploited to mediate increased cell death and suggests novel applications of FASN inhibitors for clinical use. [Mol Cancer Ther 2008;7(12):3816–24]

## Introduction

Fatty acid synthase (FASN) is the central enzyme responsible for catalyzing the ultimate steps of fatty acid synthesis in mammalian cells (1, 2). Interestingly, high levels of FASN expression have been noted in many types of tumors. Accordingly, FASN expression levels correlate with advanced tumor stage and grade, poor patient prognosis, and reduced overall and disease-free survival (3–5). A functional correlation between FASN expression levels and tumor cell survival has been firmly established with the development of small-molecule inhibitors of FASN that induce cell death specifically in tumor cells and reduce tumor growth in spontaneous and xenograft tumor models (6–10).

FASN inhibitors induce several antitumor effects including cell cycle arrest and cell death (3–5). Some of the effects of FASN inhibitors are mediated through key tumor signaling pathways. For instance, it has been shown that pharmacologic inhibition of FASN activity results in reduced Akt phosphorylation in multiple tumor cell lines (11, 12). Conversely, phosphoinositide 3-kinase and Akt can drive FASN expression in tumor cells (12, 13). The demonstration that reduced FASN activity negatively affects Akt activation identifies feedback between the two pathways. As a result, blocking both pathways results in amplified cell death (11, 12, 14). Synergy between FASN inhibitors and other chemotherapeutics has been noted in multiple cell lines (15–19). It has also been shown that FASN overexpression protects breast cancer cells from chemotherapy-induced cell death (20). The demonstrated links between FASN, oncogenic pathways, and ultimate response to chemotherapy underscore the potential of FASN inhibitors for clinical use and suggest novel strategies for targeting tumor cells to improve cell-killing efficiency.

In prostate cancer, FASN expression is stabilized by the ubiquitin-specific protease 2a, a deubiquitinating enzyme (21). Treating prostate tumor cells with the proteasome inhibitor MG-132 also increases FASN expression, supporting evidence of FASN regulation by the proteasome (21). Inhibition of the proteasome can also stabilize nuclear SREBP-1 and increase FASN expression (22). Conversely, inhibiting FASN affects the proteasome pathway. Specifically, inhibition of FASN reduces expression of the E3 ubiquitin ligase Skp2 that is responsible for mediating the stability of key cellular proteins such as p27 (23). FASN

Received 6/13/08; revised 9/16/08; accepted 9/27/08.

**Grant support:** National Cancer Institute grant 5R01CA114104-02 and Department of Defense grant W81XWH-07-1-0024 (S.J. Kridel).

The costs of publication of this article were defrayed in part by the payment of page charges. This article must therefore be hereby marked *advertisement* in accordance with 18 U.S.C. Section 1734 solely to indicate this fact.

**Requests for reprints:** Steven J. Kridel, Department of Cancer Biology, Comprehensive Cancer Center, Wake Forest University School of Medicine, Medical Center Boulevard, Winston-Salem, NC, 27157. Phone: 336-716-7299; Fax: 336-716-0255. E-mail: skridel@wfubmc.edu

Copyright © 2008 American Association for Cancer Research.

doi:10.1158/1535-7163.MCT-08-0558

inhibition also affects the expression profiles of several E2 ubiquitin conjugation enzymes and several E3 ubiquitin ligases (24). Combined, these data suggest a level of crosstalk between the FASN and proteasome pathways.

Previous work from our laboratory showed that inhibition of FASN activity induces endoplasmic reticulum (ER) stress and activation of the unfolded protein response (UPR; ref. 25). Interestingly, bortezomib (Velcade, PS-341), a Food and Drug Administration-approved inhibitor of the 26S proteasome, also activates the UPR in tumor cells (26–30). Given the connections between the proteasome and FASN, especially in prostate cancer, and that inhibitors of each induce ER stress, we hypothesized that FASN inhibitors and bortezomib could enhance prostate tumor cell death through UPR-driven mechanisms. The data presented herein show that functional crosstalk between the FASN and a proteasome pathway in prostate tumor cell lines is the basis for UPR-mediated death by two clinically relevant ER stressing agents.

## Materials and Methods

### Materials

The PC-3, DU145, and FS-4 cells were obtained from the American Type Culture Collection. Cell culture medium and supplements were from Invitrogen. Antibodies against eukaryotic translation initiation factor 2 $\alpha$  (eIF2 $\alpha$ ), phospho-eIF2 $\alpha$ , phospho-c-Jun NH<sub>2</sub>-terminal kinase (JNK), total JNK (Thr<sup>183</sup>/Tyr<sup>185</sup>), phospho-c-Jun (Ser<sup>63</sup>), lamin A/C,  $\alpha$ -tubulin, cleaved caspase-3 (Asp<sup>175</sup>), and cleaved PARP (Asp<sup>214</sup>) were from Cell Signaling Technologies. Antibody against FASN was from BD Transduction Labs. Antibody against  $\beta$ -actin was from Sigma. Antibodies against C/EBP homologous protein (CHOP; R-20), activating transcription factor 4 (ATF4; CREB2 C-20), ubiquitin (FL-76), and X-box-binding protein 1 (XBP-1; M-186) were from Santa Cruz Biotechnology. TRIzol was from Invitrogen. Avian myeloblastosis virus reverse transcriptase and Taq polymerase were from Promega. [<sup>14</sup>C]acetate was purchased from GE Healthcare. Oligonucleotides were synthesized by Integrated DNA Technologies, except for those designed for siRNA, which were synthesized by Dharmacon. Orlistat was purchased from Roche, bortezomib was purchased from Millennium Pharmaceuticals, and JNK inhibitor II, SP600125, and JNK inhibitor V, AS601245, were from Calbiochem. All other reagents were purchased from Sigma, Calbiochem, or Bio-Rad.

### Cell Culture and Drug Treatments

Prostate tumor cell lines were maintained in RPMI 1640 and FS-4 human foreskin fibroblasts were maintained in DMEM-high glucose, both supplemented with 10% fetal bovine serum at 37°C and 5% CO<sub>2</sub>. Cells were treated for the times and with drug concentrations as indicated. Orlistat was extracted from capsules in ethanol as described previously and stored at –80°C (8). Further dilutions were made in DMSO. Bortezomib was dissolved in DMSO and stored as individual 20  $\mu$ mol/L aliquots at –20°C.

### Immunoblot Analysis

Cells were harvested after the indicated treatments, washed with ice-cold PBS, and lysed in buffer containing 1% Triton X-100 to prepare for immunoblots. Lysis buffer was supplemented with protease, kinase, and phosphatase inhibitors 200  $\mu$ mol/L phenylmethylsulfonyl fluoride, 5  $\mu$ g/mL aprotinin, 5  $\mu$ g/mL pepstatin A, 5  $\mu$ g/mL leupeptin, 1  $\mu$ mol/L sodium fluoride, 1  $\mu$ mol/L sodium orthovanadate, and 50  $\mu$ mol/L okadaic acid just before use. For nuclear proteins, such as ATF4, CHOP, and XBP-1, nuclear extracts were obtained by harvesting cells, washing with ice-cold PBS, and then lysing cells using a harvest buffer containing 10 mmol/L HEPES (pH 7.9), 50 mmol/L NaCl, 500 mmol/L sucrose, 100  $\mu$ mol/L EDTA, 0.5% Triton X-100 with 1 mmol/L DTT, 10 mmol/L tetrasodium pyrophosphate, 100 mmol/L sodium fluoride, 17.5 mmol/L  $\beta$ -glycerophosphate, 1  $\mu$ mol/L sodium orthovanadate, 1 mmol/L phenylmethylsulfonyl fluoride, 4  $\mu$ g/mL aprotinin, and 2  $\mu$ g/mL pepstatin A added just before use to separate the cytoplasmic and nuclei. The nuclei were pelleted in a swinging bucket rotor and then washed with buffer containing 10 mmol/L HEPES (pH 7.9), 10 mmol/L KCl, 100  $\mu$ mol/L EDTA, and 100  $\mu$ mol/L EGTA with 1 mmol/L DTT, 1 mmol/L phenylmethylsulfonyl fluoride, 1  $\mu$ mol/L sodium orthovanadate, 4  $\mu$ g/mL aprotinin, and 2  $\mu$ g/mL pepstatin added just before use. The nuclei were then lysed in a buffer containing 10 mmol/L HEPES (pH 7.9), 500 mmol/L NaCl, 100  $\mu$ mol/L EDTA, 100  $\mu$ mol/L EGTA, and 0.1% NP-40 with 1 mmol/L DTT, 1 mmol/L phenylmethylsulfonyl fluoride, 1  $\mu$ mol/L sodium orthovanadate, 4  $\mu$ g/mL aprotinin, and 2  $\mu$ g/mL pepstatin added just before use. Protein samples were electrophoresed through 10%, 12%, or 13.5% SDS-polyacrylamide gels and transferred to nitrocellulose, except for blots to detect phospho-eIF2 $\alpha$  and eIF2 $\alpha$ , which were transferred to Immobilon-P membrane (polyvinylidene difluoride). Immunoreactive bands were detected by enhanced chemiluminescence (Perkin-Elmer). Lamin A/C and  $\beta$ -actin were used as loading controls for immunoblots.

### Quantification of Ubiquitin-Modified Proteins

Autoradiographs were scanned using a HP ScanJet4890. The digital files were then quantified using UN-SCAN-IT. The average intensity of ubiquitin detection was calculated relative to vehicle-treated samples for each blot. Then, the values for three independent experiments were averaged and graphed on a logarithmic scale.

### Fatty Acid Synthesis Assays

To measure fatty acid synthesis,  $1 \times 10^5$  cells per well were seeded in 24-well plates. Cells were treated with FASN inhibitors or bortezomib as indicated for 2 h. [<sup>14</sup>C]acetate (1  $\mu$ Ci) was added to each well for an additional 2 h. Cells were collected and washed and lipids were extracted and quantified by scintillation counting as described previously (8).

### Clonogenic Survival Assays

PC-3 and DU145 cells were plated in 6-well plates at a density of 2,000 per well 48 h before each experiment. Fresh medium containing the indicated drugs was added at the

indicated concentrations for 16 h. The medium was then removed, the wells were washed, and fresh medium was added. Plates were incubated until macroscopic colonies were formed. Visualization of colonies was done as described previously (25). Colonies were quantified by counting.

#### Combination Index and Statistical Calculations

PC-3 cells were treated with a dose response of orlistat, bortezomib, or the combination and analyzed for clonogenic survival. Calculations were done based on the Chou-Talalay method that calculates a combination index based on the equation: combination index =  $(D1) / (Dx1) + (D2) / (Dx2) + (D1)(D2) / (Dx1)(Dx2)$ , where (D1) and (D2) are the doses of the individual drugs that have "x" effect when used in combination and (Dx1) and (Dx2) are the doses of the drugs having "x" effect when used separately (31). A combination index < 1 indicates synergism.

For clonogenic survival assays, survival of treated cells was normalized relative to vehicle-treated cells and *P* values between combined and single-agent treated cells were determined by two-tailed Student's *t* tests. For fatty acid synthesis assays, bortezomib-treated cells were compared with vehicle-treated cells and *P* values were determined by two-tailed Student's *t* test. For the ubiquitin modification blots, the quantification of three separate blots was averaged for each treatment and then significance measured relative to untreated controls by two-tailed Student's *t* test.

#### Detection of XBP-1 Splicing and GADD34 Expression and Suppression of CHOP Expression with siRNA

Cells were exposed to the various drug treatments or transfected with siRNA for the indicated times. Reverse transcription-PCR was done for XBP-1 splicing and GADD34 expression as described previously (25). To knockdown CHOP levels, a siGENOME SMARTpool siRNA oligonucleotide cocktail against *CHOP* (1, AAAU-GAAGAGGAAGAAUCA; 2, GAAUCUGCACCAAGCAUGA; 3, CCAGCAGAGGUCACAAGCA; and 4, GAGCUCUGAUUGACCGAAU) and one control siRNA against luciferase as a negative control (Luc sense, CUUACGUGAUACUUCGAUU) were designed and synthesized by Dharmacon. The individual siRNAs (83 nmol/L) were transfected into cells at plating with siPORT *NeoFX* transfection reagent (Ambion) according to manufacturer's instructions. After 48 h, transfection medium was removed and fresh medium containing indicated drug was added to cells. After indicated treatment times, cells were collected and nuclear protein was harvested for immunoblot analysis of CHOP and lamin A/C or tubulin.

## Results

We hypothesized that the identified connections between the fatty acid synthesis and proteasome pathways would provide a novel strategy to target UPR activation and

increase cell death in prostate tumor cells. To test this hypothesis, PC-3 and DU145 cells were examined for clonogenic survival after treatment with orlistat or C75 and the proteasome inhibitor bortezomib. Clonogenic survival of PC-3 and DU145 cells was reduced by bortezomib treatment in a dose-dependent manner (Fig. 1A and B). Suboptimal concentrations of FASN inhibitors were used to reduce cell killing by any of the single agents (data not

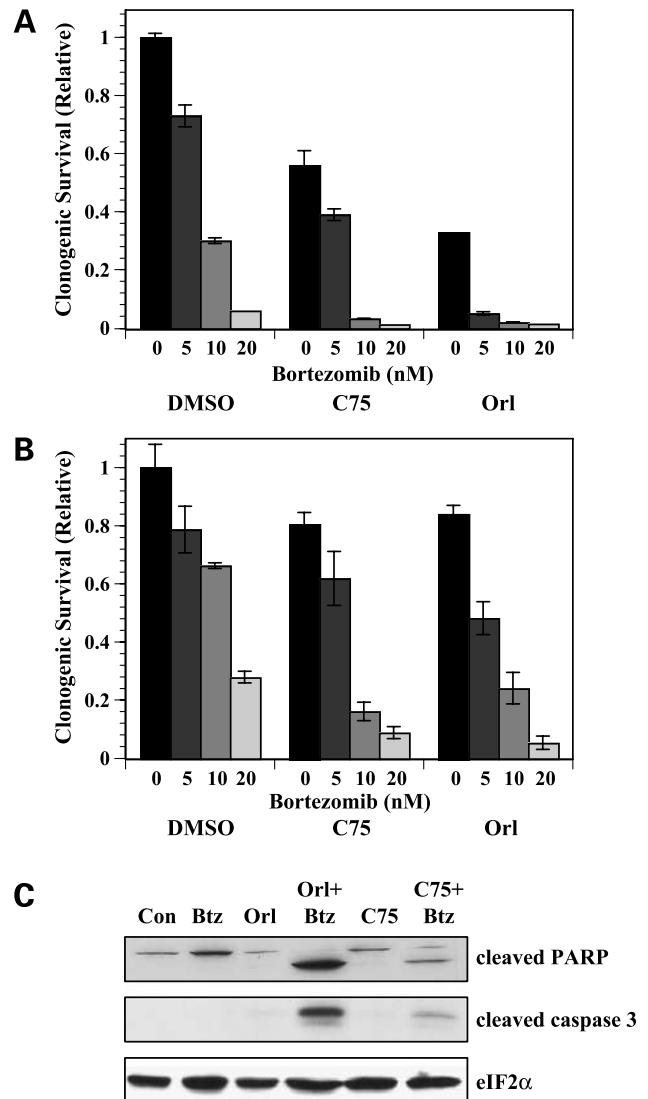


**Figure 1.** FASN inhibitors combine with bortezomib to increase cell death. Clonogenic survival assays were done on PC-3 (A) and DU145 (B) cells. Cells were treated with the indicated concentrations of bortezomib in the presence of DMSO, C75 (10  $\mu$ g/mL), or orlistat (25  $\mu$ mol/L) for 16 h. Clonogenic survival was determined relative to vehicle-treated controls. Statistical significance was determined by two-tailed Student's *t* test of cells treated with the combination of FASN inhibitors and bortezomib compared with cells treated with FASN inhibitors alone ( $P \leq 0.005$ ). C, PC-3 cells treated with bortezomib (5 nmol/L), orlistat (25  $\mu$ mol/L), C75 (10  $\mu$ g/mL), or the combination of FASN inhibitors and bortezomib for 18 h and collected for immunoblot analysis using antibodies specific for cleaved PARP, cleaved caspase 3, and total eIF2 $\alpha$ . Images represent cropped immunoblots. Full-length scans available in Supplementary Fig. S1.<sup>1</sup>

<sup>1</sup>Supplementary material for this article is available at Molecular Cancer Therapeutics Online (<http://mct.aacrjournals.org/>).

shown). Clonogenic survival of PC-3 cells treated with orlistat and C75 was reduced by 60% and 30%, respectively ( $P < 0.001$ ; Fig. 1A). In DU145 cells, survival was only reduced by ~20% with each inhibitor. When the FASN inhibitors were combined with bortezomib, clonogenic survival was strikingly diminished compared with cells treated with the single agents ( $P \leq 0.005$ ; Fig. 1A and B). Although isobologram analyses were inconclusive, an analysis of the combination index suggests that combining FASN inhibitors with bortezomib results in synergism (31). Consistent with previous findings, suboptimal concentrations of orlistat and C75 did not result in cleavage of PARP or caspase-3. However, when FASN inhibitors were combined with bortezomib, significant levels of both cleaved PARP and cleaved caspase-3 were detected (Fig. 1C). Combined, the data showed that combining bortezomib and FASN inhibitors resulted in enhanced cell death.

Given the established links between the fatty acid synthesis and proteasome pathways, we asked whether inhibition of FASN would affect the function of the proteasome. PC-3 cells were treated with FASN inhibitors, bortezomib, or FASN inhibitors and bortezomib together

followed by immunoblot analysis of ubiquitin-modified proteins. As expected, bortezomib induced accumulation of ubiquitin-modified proteins ( $P \leq 0.05$ ; Fig. 2A and B). Interestingly, PC-3 cells treated with orlistat or C75 also induced a modest but significant accumulation of ubiquitin-modified proteins ( $P \leq 0.01$ ). The cotreatment of FASN inhibitors with bortezomib also appeared to cause an additive accumulation of ubiquitin-modified proteins (Fig. 2A and B), further suggesting that FASN activity contributes to the functionality of the proteasomal pathway. Next, we asked whether bortezomib affected fatty acid synthesis. Bortezomib induced a dose-dependent increase in fatty acid synthesis in PC-3 cells and a modest but significant increase in DU145 cells ( $P \leq 0.05$ ; Fig. 2C). On the other hand, bortezomib had no effect on fatty acid synthesis in FS-4 human fibroblasts. The increased fatty acid synthesis was not associated with increased FASN protein levels (Fig. 2D). Collectively, these data show crosstalk between the FASN and proteasome pathways.

Previous work showed that FASN inhibitors induce ER stress in tumor cells and others have shown that bortezomib induces ER stress (25, 28–30, 32). To characterize the role of the UPR in cells treated with the combination of

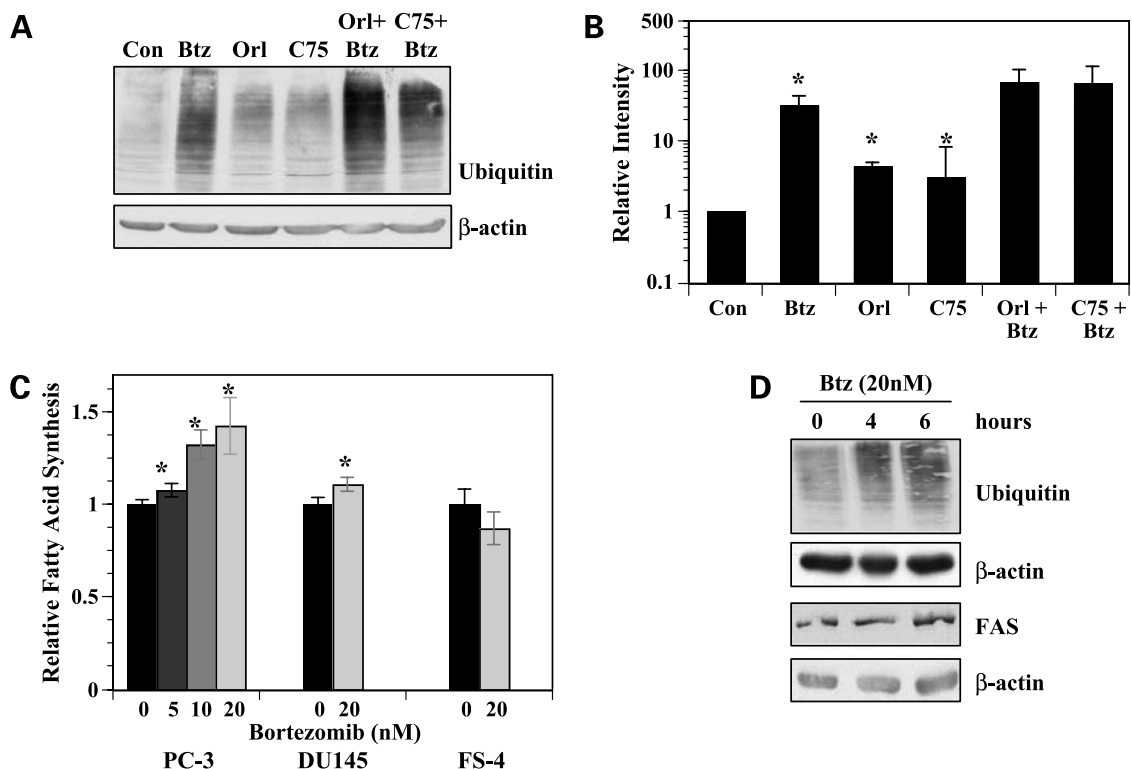


**Figure 2.** Fatty acid synthesis and proteasome pathways exhibit crosstalk. **A**, PC-3 cells were treated with vehicle, orlistat (25  $\mu$ mol/L), bortezomib, (5 nmol/L), C75 (9  $\mu$ g/mL), or the combination of bortezomib and orlistat or C75 for 16 h and subjected to immunoblot analysis with antibodies specific for ubiquitin and  $\beta$ -actin. **B**, three separate experiments of PC-3 cells treated as in **A** were quantified by measuring intensity of the exposure from ubiquitin antibody in each treatment as compared with vehicle-treated lanes using UN-SCAN-IT. \*,  $P \leq 0.05$ , Student's *t* test. **C**, PC-3 cells, DU145 cells, and FS-4 fibroblasts were incubated with the indicated concentrations of bortezomib for 2 h followed by the addition of [ $^{14}$ C]acetate (1  $\mu$ Ci) for 2 h. Cells were collected and washed and lipids were extracted and quantified relative to vehicle-treated control as described in Materials and Methods. \*,  $P \leq 0.05$ , Student's *t* test. **D**, PC-3 cells were treated with vehicle or bortezomib (20 nmol/L) for 4 or 6 h in duplicate. Cells were collected for immunoblot analysis using antibodies specific to FASN, ubiquitin, or  $\beta$ -actin. Images represent cropped immunoblots. Full-length scans available in Supplementary Fig. S2.

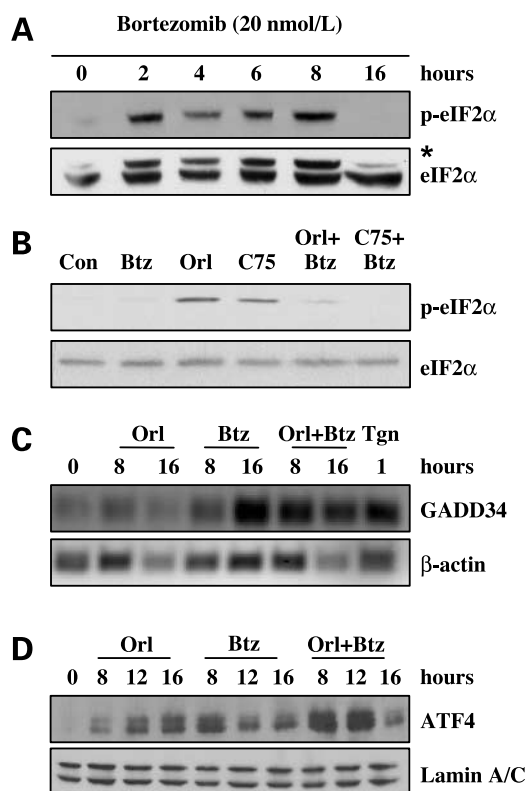


**Figure 3.** Bortezomib and FASN inhibitors combine to saturate the PERK arm of UPR adaptation signaling. **A**, PC-3 cells were treated with vehicle (DMSO) or 20 nmol/L bortezomib for the indicated times. Samples were resolved by SDS-PAGE and transferred to polyvinylidene difluoride and the membrane was probed with antibodies specific for phospho-eIF2 $\alpha$  and total eIF2 $\alpha$ . **B**, PC-3 cells were treated with vehicle, bortezomib (5 nmol/L), orlistat (25  $\mu$ mol/L), C75 (10  $\mu$ g/mL), or the combination of bortezomib and orlistat or bortezomib and C75 for 16 h and samples were subjected to immunoblot analysis and probed with antibodies specific for phospho-eIF2 $\alpha$  and total eIF2 $\alpha$ . Asterisk, higher molecular weight nonspecific band. **C**, PC-3 cells were treated with vehicle, orlistat (25  $\mu$ mol/L), bortezomib (20 nmol/L), or the combination of bortezomib and orlistat for the indicated times. Total RNA was collected and semiquantitative reverse transcription-PCR was done using primers specific for GADD34 and  $\beta$ -actin. **D**, PC-3 cells were treated with vehicle, orlistat (25  $\mu$ mol/L), bortezomib (5 nmol/L), or the combination of bortezomib and orlistat. Nuclear fractions were isolated and prepared for immunoblot analysis and probed with antibodies specific for ATF4 and lamin A/C. Images represent cropped immunoblots. Full-length scans available in Supplementary Fig. S3.

FASN inhibitors and bortezomib, we first examined the phosphorylation status of eIF2 $\alpha$ . Bortezomib induced a rapid and transient phosphorylation of eIF2 $\alpha$  that diminished by 16 h (Fig. 3A). Consistent with previous findings, phosphorylation of eIF2 $\alpha$  was sustained through 16 h in cells treated with FASN inhibitor (25). Disrupting the crosstalk between the proteasome and FASN resulted in non-phospho-eIF2 $\alpha$  at 16 h, consistent with the lack of phospho-eIF2 $\alpha$  with bortezomib alone at the same time point (Fig. 3B).

In the UPR signaling cascade, growth arrest and DNA damage-inducible protein 34 (GADD34) is induced, mediating dephosphorylation of eIF2 $\alpha$  to restore bulk transla-

tion (33, 34). To test whether single and combined agents induce GADD34 expression over the course of 16 h, semiquantitative reverse transcription-PCR was done with oligonucleotides specific for GADD34. PC-3 cells treated with orlistat showed slight GADD34 mRNA at 8 and 16 h compared with vehicle-treated controls (Fig. 3C). Consistent with the time course of eIF2 $\alpha$  phosphorylation in bortezomib-treated cells, GADD34 mRNA expression was minimal at 8 h followed by robust expression at 16 h (Fig. 3C). Inhibiting crosstalk between pathways induced GADD34 mRNA expression by 8 h to a level higher than seen with bortezomib or orlistat alone that was maintained through 16 h, correlating with the lack of phospho-eIF2 $\alpha$  at the same time point (Fig. 3C). Together, these data showed that interrupting crosstalk between the proteasome and FASN resulted in acceleration of the eIF2 $\alpha$ -GADD34 feedback loop indicative of increased UPR signaling and suggested that proteotoxicity may contribute to cell death.

Phosphorylation of eIF2 $\alpha$  is a primary event in UPR signaling that activates downstream signals including the prosurvival ATF4 (35, 36). Therefore, we tested whether interrupting crosstalk between proteasome and fatty acid synthesis pathways would increase ATF4 expression. Orlistat induced early expression of ATF4 at 8 h that was sustained through the 16 h time point (Fig. 3D), consistent with robust phosphorylation of eIF2 $\alpha$  (Fig. 3B) and low levels of GADD34 (Fig. 3C) in orlistat-treated cells. Bortezomib treatment induced expression of nuclear ATF4 by 8 h, which decreased at 12 and 16 h, consistent with phospho-eIF2 $\alpha$  status and GADD34 expression (Fig. 3). Interfering with the FASN-proteasome crosstalk induced ATF4 expression that was more robust than orlistat- or bortezomib-treated cells at 8 h but decreased by the 16 h time point (Fig. 3D). Correspondingly, GADD34 levels were high and phospho-eIF2 $\alpha$  levels were low at 16 h in combination-treated cells (Fig. 3C). Together, the time courses of eIF2 $\alpha$  phosphorylation, GADD34, and ATF4 expression indicated that adaptation signals of the PERK arm of the UPR pathway was not only active in cells treated with FASN inhibitors and bortezomib but was saturated when both pathways were inhibited.

We next examined the IRE1-mediated processing of XBP-1 in cells treated with orlistat, bortezomib, or both. Suboptimal concentrations of orlistat and bortezomib induced moderate splicing of XBP-1 mRNA by 8 h (Fig. 4A). Treating cells with both agents caused an earlier and more robust processing of XBP-1 that was complete by 16 h (Fig. 4A). Correspondingly, at these times and concentrations, accumulation of the XBP-1(s) transcription factor only occurred in cells treated with both FASN inhibitor and bortezomib (Fig. 4B and C). Therefore, interfering with FASN and the proteasome simultaneously enhanced the adaptation response through IRE1-mediated processing of XBP-1 in prostate tumor cells.

We next asked whether IRE1-activated signals characteristic of the alarm arm of the UPR pathway were up-regulated in cells in which we inhibited fatty acid

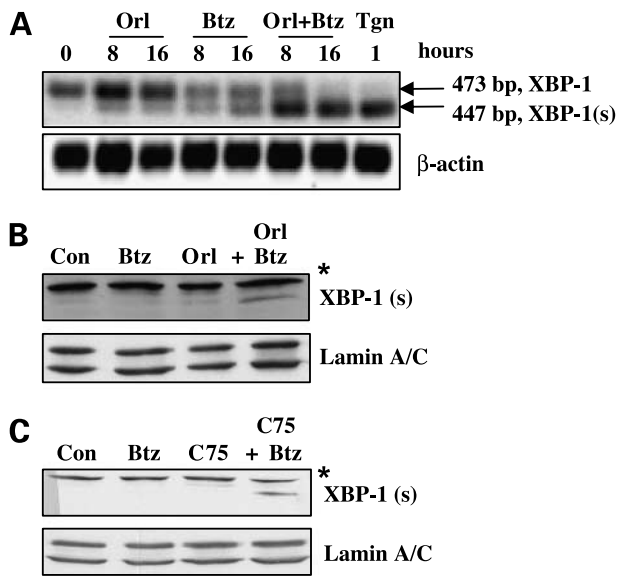


**Figure 4.** Combining bortezomib with FASN inhibitors enhances IRE1-mediated XBP-1 mRNA processing. **A**, PC-3 cells were treated with vehicle, orlistat (25  $\mu\text{mol/L}$ ), bortezomib (5 nmol/L), or the combination of bortezomib and orlistat. Total RNA was collected with TRIzol and reverse transcription-PCR was done with oligonucleotides specific for XBP-1 and  $\beta$ -actin. XBP-1(us) is indicated by the 473 bp product and XBP-1(s) is indicated by the 447 bp fragment. PC-3 cells were treated for 1 h with thapsigargin (1  $\mu\text{mol/L}$ ) as a positive control. **B**, PC-3 cells were treated with vehicle, orlistat (25  $\mu\text{mol/L}$ ), bortezomib (5 nmol/L), or the combination of bortezomib and orlistat. Nuclear lysates were collected as described in Materials and Methods for immunoblot analysis with antibodies specific for XBP-1 and lamin A/C. Immunoblot indicates the 55 kDa XBP-1(s) protein. *Asterisk*, higher molecular weight nonspecific band. **C**, PC-3 cells were treated with vehicle, bortezomib (5 nmol/L), C75 (9  $\mu\text{g/mL}$ ), or the combination of bortezomib and C75. *Asterisk*, higher molecular weight nonspecific band. Images represent cropped immunoblots. Full-length scans available in Supplementary Fig. S4.

synthesis-proteasome crosstalk. The phosphorylation status of JNK was examined by immunoblot (Fig. 5A). Orlistat did not induce JNK phosphorylation, and bortezomib treatment induced only minimal JNK activation at 16 h (Fig. 5A). Treating cells with both agents in combination, though, induced JNK phosphorylation within 4 h that increased through 16 h. Similar results were observed in DU145 cells (data not shown). The CHOP transcription factor can be induced by JNK activation (37, 38). Orlistat only induced moderate CHOP expression at 16 h (Fig. 5B). Similarly, at 12 h, bortezomib induced minimal CHOP expression that slightly increased by 16 h (Fig. 5B). On the other hand, combined inhibition of FASN and the proteasome pathways induced an earlier and more robust CHOP expression (Fig. 5B). A JNK inhibitor was used to verify the role of JNK in mediating CHOP expression. Pharmacologic inhibition of JNK blocked the phosphorylation of JNK and c-Jun (Fig. 6A). More importantly, inhibition of JNK also reduced CHOP expression and cleavage of caspase-3 and PARP (Fig. 6A). Consistent with these findings, trypan blue exclusion assays also showed that JNK inhibition protected cells from cell death induced

by the combination of orlistat and bortezomib ( $P < 0.01$ ; Fig. 6B).

We next tested whether CHOP is an effector of JNK signaling that regulates cell death in this scenario. PC-3 cells were transfected with control or *CHOP*-targeted siRNA, and after 48 h, the cells were treated with vehicle, orlistat, or the orlistat-bortezomib combination. The siRNA-mediated knockdown of *CHOP* had no effect on orlistat- or bortezomib-induced cell death (not shown). However, siRNA-mediated knockdown of *CHOP* expression protected cells from the effects of the orlistat-bortezomib combination ( $P < 0.01$ ; Fig. 6C) at a level that was proportional with the reduction in *CHOP* levels (Fig. 6D). Therefore, it appears that the JNK-CHOP axis is an important mediator of cell death in cells where the UPR is saturated. Collectively, these data show that blocking crosstalk between FASN and the proteasome shifts UPR balance from adaptation phase to the alarm phase, resulting in increased cell death via JNK-mediated *CHOP* expression.

## Discussion

We have shown previously that inhibiting FASN induces ER stress and UPR signaling before cell death occurs and hypothesize that cell death induced by FASN inhibition is dependent on UPR activation (25). The data herein reveal a functional nexus between FASN and the proteasome. The connection of each of these pathways with ER homeostasis provides a unique therapeutic opportunity. Indeed, when inhibitors of both the proteasome and FASN pathways are combined, increased cell death occurs through the IRE1-JNK-CHOP arm of the UPR pathway.

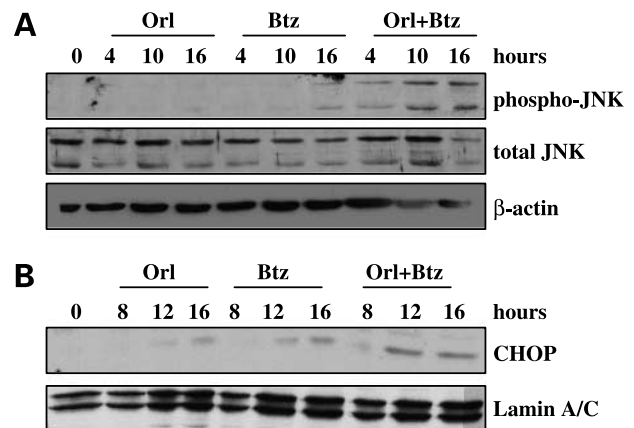


**Figure 5.** Combining bortezomib and FASN inhibitors induces JNK activation and CHOP expression. **A**, PC-3 cells were treated with vehicle, orlistat (25  $\mu\text{mol/L}$ ), bortezomib (20 nmol/L), or the combination of bortezomib and orlistat for the indicated times. Whole-cell lysates were collected for immunoblot analysis of phospho-JNK, total JNK, and  $\beta$ -actin. **B**, PC-3 cells were treated with vehicle, orlistat (25  $\mu\text{mol/L}$ ), bortezomib (20 nmol/L), or the combination of bortezomib and orlistat for the indicated times. Nuclear lysates were collected as described in Materials and Methods for immunoblot analysis with antibodies specific for CHOP and lamin A/C. Images represent cropped immunoblots. Full-length scans available in Supplementary Fig. S5.

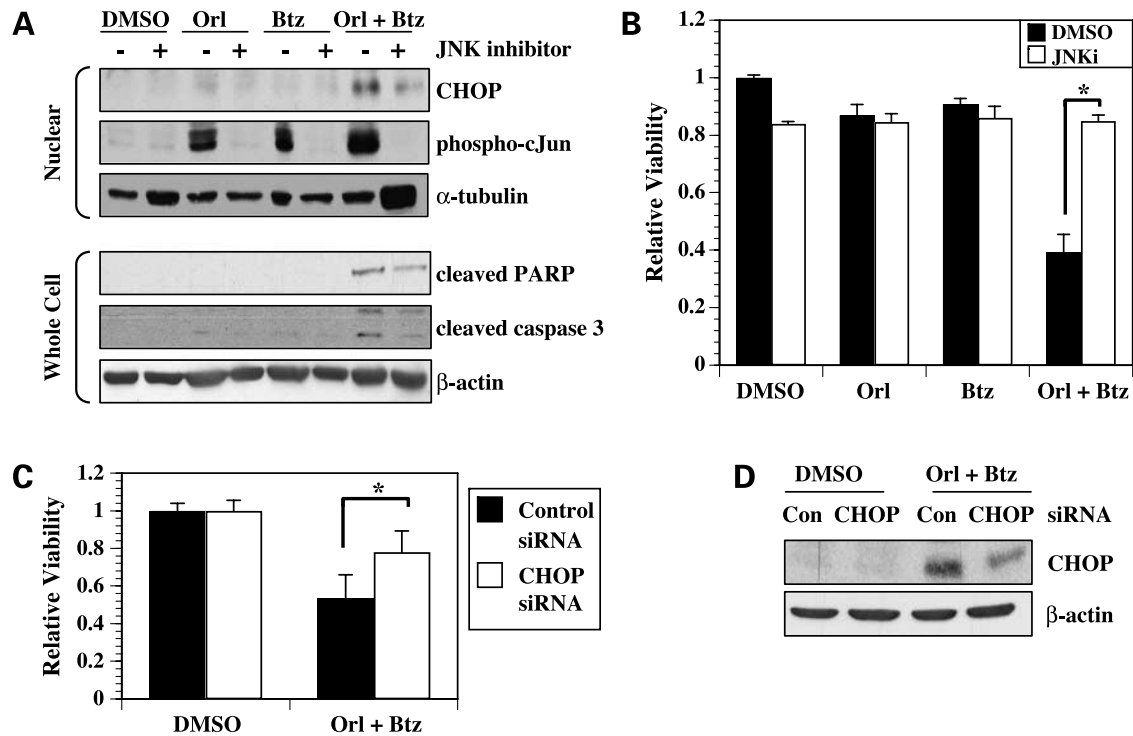


**Figure 6.** UPR-associated cell death is mediated by JNK activation and CHOP. **A**, PC-3 cells were treated with vehicle, orlistat (50  $\mu$ mol/L), bortezomib (20 nmol/L), or the combination of bortezomib and orlistat with and without JNK inhibitor (*JNKi*; 20 nmol/L). Nuclear lysates were collected as described in Materials and Methods for immunoblot analysis with antibodies specific for CHOP, phospho-c-Jun, and  $\alpha$ -tubulin. Whole-cell lysates were analyzed with antibodies specific for cleaved PARP, cleaved caspase 3, and  $\beta$ -actin. **B**, PC-3 cells were treated with vehicle, orlistat (50  $\mu$ mol/L), bortezomib (20 nmol/L), or the combination of bortezomib and orlistat with and without JNK inhibitor (20 nmol/L). Cells were collected and counted using a trypan blue exclusion assay and the ratio of viable cells was calculated relative to vehicle-treated cells. \*,  $P < 0.01$ , Student's *t* test. **C**, PC-3 cells were transfected with a SMARTpool siRNA against CHOP or a control siRNA. After 48 h, cells were treated with vehicle or the combination of bortezomib (20 nmol/L) and orlistat (50  $\mu$ mol/L) for 18 h. Cells were then collected and counted using trypan blue exclusion and the ratios of viable cells relative to vehicle-treated controls were calculated from three independent experiments. Statistical significance between CHOP siRNA and control siRNA cells treated with orlistat and bortezomib was determined by two-tailed Student's *t* test ( $P < 0.01$ ). **D**, cells from **C** were analyzed by immunoblot with antibodies specific for CHOP and  $\beta$ -actin. Images represent cropped immunoblots. Full-length scans available in Supplementary Fig. S6.

Accumulating evidence links the proteasome and FASN pathways (21, 23, 24). The data herein suggest that the integrity of the proteasome pathway relies, at least in part, on functional fatty acid synthesis, as FASN inhibitors cause the accumulation of ubiquitinated proteins through an undetermined mechanism (Fig. 2). It is possible that either the proteasome overall or a component of the proteasome pathway relies on the fatty acid synthesis pathway for proper function. Interestingly, the ER stressor tunicamycin can also induce the accumulation of ubiquitin-modified proteins and enhances the stability of E3 ligases gp78 and Hrd1 (39). Therefore, it is likely that the proper functioning of proteasome-mediated ER-associated degradation pathway is dependent on global ER function.

Perhaps more interesting is that inhibiting the proteasome alone can increase fatty acid synthesis (Fig. 2C). As the increased activity does not correlate with increased FASN protein levels, the data suggest a mechanism independent of SREBP-1 or FASN protein stabilization as others have shown previously (21, 22). Induction of fatty acid synthesis by bortezomib could be due to several

possibilities. Inhibition of the proteasome could affect turnover of a protein that modifies FASN or acetyl-CoA carboxylase. Because of the short time of treatment with bortezomib required to detect the increase of lipogenesis, a previously unidentified post-translational modification may occur to increase activity of either FASN or acetyl-CoA carboxylase. Alternatively, there could be increased incorporation of fatty acid into phospholipid. Previous studies have shown that XBP-1(s) can increase phosphatidylcholine synthesis (40). However, significant splicing of XBP-1 was not observed within the same period in which fatty acid synthesis increased (Fig. 4). Therefore, it is unlikely that XBP-1(s) induces phospholipid synthesis in response to bortezomib treatment. Regardless, the crosstalk between FASN and proteasome pathways is the basis for amplification of UPR signaling and increased cell death when inhibitors of these pathways are combined. Increased UPR signaling in this scenario, particularly that of the alarm arm, supports a growing body of literature describing the ability for the UPR to induce cell death after adaptation signals have been saturated or are ineffective (41–43).

The activation of adaptation and stress signals is critical to the cellular balance between survival and cell death. PERK-dependent phosphorylation of eIF2 $\alpha$  can act as a rheostat to fine-tune signals that balance survival and death in a cell experiencing ER stress (44). If a cell is unable to sustain balanced levels of phospho-eIF2 $\alpha$ , the cell dies due to proteotoxicity. If the cell has levels of phospho-eIF2 $\alpha$  that are too high, the cell cannot translate enough protein to adapt and survive. Compared with the combination of FASN inhibitors with bortezomib and bortezomib alone, FASN inhibitors take the longest amount of time to induce cell death. Correspondingly, FASN inhibitors result in sustained phospho-eIF2 $\alpha$ , therefore more cellular protection (Fig. 3). Simultaneous inhibition of the proteasome and fatty acid synthesis pathways induces early and robust GADD34 expression to mediate the dephosphorylation of eIF2 $\alpha$  (Fig. 3). Coincidentally, the combined treatment quickly induces cell death perhaps by proteotoxicity associated with decreased eIF2 $\alpha$  phosphorylation.

The IRE1 arm of the UPR is another signaling pathway designed to mediate adaptation and alarm signals (41, 43, 45). IRE1 splices XBP-1 mRNA that is then translated to a stable ER stress-specific transcription factor that up-regulates ER chaperones and other adaptation genes (46, 47). We show that FASN inhibitors and bortezomib both induce splicing of XBP-1 but that the combined treatment results in the accumulation of the XBP-1 transcription factor (Fig. 4A-C). Therefore, blockade of FASN-proteasome crosstalk enhances adaptation signaling through the IRE1 arm of the UPR. Inhibiting both pathways also shifts the balance from adaptation to stress signaling downstream of IRE1. Activated IRE1 can also interact with tumor necrosis factor receptor adaptor factor 2 to activate JNK and corresponding alarm signals, including expression of the ER stress proapoptotic protein CHOP (38, 48). Indeed, the combined treatment results in robust activation of JNK as well as enhanced accumulation of CHOP, thereby confirming the hypothesis that increased ER stress shifts the UPR program to cell death. Consistent with other studies, the data presented here indicate that CHOP mediates cell death when FASN-proteasome crosstalk is interrupted (Fig. 6; ref. 49). That JNK and CHOP mediate death in this system is consistent with the notion that IRE1 guides cell fate in response to ER stress (43).

Altogether, the data indicate that rapid and robust UPR activation occurs when FASN and the proteasome are inhibited simultaneously. Although the connection between the proteasome and the ER-associated degradation pathway has been established, the mechanism by which FASN mediates proteasome function remains to be determined. It will be important for future studies to determine the precise connections between these two important tumor support systems. Significant interest and opportunity lies in exploiting the UPR with therapeutic agents to augment tumor cell death. Collectively, these data provide insight into how FASN and the proteasome can be targeted to shift UPR balance from adaptation to stress signaling to affect increased tumor cell death.

## Disclosure of Potential Conflicts of Interest

No potential conflicts of interest were disclosed.

## References

- Jayakumar A, Tai MH, Huang WY, et al. Human fatty acid synthase: properties and molecular cloning. *Proc Natl Acad Sci U S A* 1995;92:8695–9.
- Wakil SJ, Stoops JK, Joshi VC. Fatty acid synthesis and its regulation. *Annu Rev Biochem* 1983;52:537–79.
- Kridel SJ, Lowther WT, Pemble CW. Fatty acid synthase inhibitors: new directions for oncology. *Expert Opin Investig Drugs* 2007;16:1817–29.
- Kuhajda FP. Fatty-acid synthase and human cancer: new perspectives on its role in tumor biology. *Nutrition* 2000;16:202–8.
- Kuhajda FP. Fatty acid synthase and cancer: new application of an old pathway. *Cancer Res* 2006;66:5977–80.
- Funabashi H, Kawaguchi A, Tomoda H, et al. Binding site of cerulenin in fatty acid synthetase. *J Biochem (Tokyo)* 1989;105:751–5.
- Kuhajda FP, Pizer ES, Li JN, et al. Synthesis and antitumor activity of an inhibitor of fatty acid synthase. *Proc Natl Acad Sci U S A* 2000;97:3450–4.
- Kridel SJ, Axelrod F, Rozenkrantz N, Smith JW. Orlistat is a novel inhibitor of fatty acid synthase with antitumor activity. *Cancer Res* 2004;64:2070–5.
- Alli PM, Pinn ML, Jaffee EM, McFadden JM, Kuhajda FP. Fatty acid synthase inhibitors are chemopreventive for mammary cancer in neu-N transgenic mice. *Oncogene* 2005;24:39–46.
- Zhou W, Han WF, Landree LE, et al. Fatty acid synthase inhibition activates AMP-activated protein kinase in SKOV3 human ovarian cancer cells. *Cancer Res* 2007;67:2964–71.
- Wang HQ, Altomare DA, Skele KL, et al. Positive feedback regulation between AKT activation and fatty acid synthase expression in ovarian carcinoma cells. *Oncogene* 2005;24:3574–82.
- Liu X, Shi Y, Giranda VL, Luo Y. Inhibition of the phosphatidylinositol 3-kinase/Akt pathway sensitizes MDA-MB468 human breast cancer cells to cerulenin-induced apoptosis. *Mol Cancer Ther* 2006;5:494–501.
- Van de Sande T, De Schrijver E, Heyns W, Verhoeven G, Swinnen JV. Role of the phosphatidylinositol 3'-kinase/PTEN/Akt kinase pathway in the overexpression of fatty acid synthase in LNCaP prostate cancer cells. *Cancer Res* 2002;62:642–6.
- Bandyopadhyay S, Pai SK, Watabe M, et al. FAS expression inversely correlates with PTEN level in prostate cancer and a PI 3-kinase inhibitor synergizes with FAS siRNA to induce apoptosis. *Oncogene* 2005;24:5389–95.
- Menendez JA, Vellon L, Mehmi I, et al. Inhibition of fatty acid synthase (FAS) suppresses HER2/neu (erbB-2) oncogene overexpression in cancer cells. *Proc Natl Acad Sci U S A* 2004;101:10715–20.
- Menendez JA, Vellon L, Lupu R. Antitumoral actions of the anti-obesity drug orlistat (Xenical<sup>TM</sup>) in breast cancer cells: blockade of cell cycle progression, promotion of apoptotic cell death and PEA3-mediated transcriptional repression of Her2/neu (erbB-2) oncogene. *Ann Oncol* 2005;16:1253–67.
- Menendez JA, Colomer R, Lupu R. Inhibition of tumor-associated fatty acid synthase activity enhances vinorelbine (Navelbine)-induced cytotoxicity and apoptotic cell death in human breast cancer cells. *Oncol Rep* 2004;12:411–22.
- Menendez JA, Lupu R, Colomer R. Inhibition of tumor-associated fatty acid synthase hyperactivity induces synergistic chemosensitization of HER-2/neu-overexpressing human breast cancer cells to docetaxel (Taxotere). *Breast Cancer Res Treat* 2004;84:183–95.
- Menendez JA, Vellon L, Colomer R, Lupu R. Pharmacological and small interference RNA-mediated inhibition of breast cancer-associated fatty acid synthase (oncogenic antigen-519) synergistically enhances Taxol (paclitaxel)-induced cytotoxicity. *Int J Cancer* 2005;115:19–35.
- Liu H, Liu Y, Zhang J-T. A new mechanism of drug resistance in breast cancer cells: fatty acid synthase overexpression-mediated palmitate overproduction. *Mol Cancer Ther* 2008;7:263–70.
- Graner E, Tang D, Rossi S, et al. The isopeptidase USP2a regulates the stability of fatty acid synthase in prostate cancer. *Cancer Cell* 2004;5:253–61.

22. Hirano Y, Yoshida M, Shimizu M, Sato R. Direct demonstration of rapid degradation of nuclear sterol regulatory element-binding proteins by the ubiquitin-proteasome pathway. *J Biol Chem* 2001;276:36431–7.
23. Knowles LM, Axelrod F, Browne CD, Smith JW. A fatty acid synthase blockade induces tumor cell-cycle arrest by down-regulating Skp2. *J Biol Chem* 2004;279:30540–5.
24. Knowles LM, Smith JW. Genome-wide changes accompanying knockdown of fatty acid synthase in breast cancer. *BMC Genomics* 2007;8:168–81.
25. Little JL, Wheeler FB, Fels DR, Koumenis C, Kridel SJ. Inhibition of fatty acid synthase induces endoplasmic reticulum stress in tumor cells. *Cancer Res* 2007;67:1262–9.
26. Alberts B, Johnson A, Lewis J, et al., editors. *Molecular biology of the cell*. 4th ed. New York: Garland Science; 2002.
27. Gardner RC, Assinder SJ, Christie G, et al. Characterization of peptidyl boronic acid inhibitors of mammalian 20S and 26S proteasomes and their inhibition of proteasomes in cultured cells. *Biochem J* 2000;346:447–54.
28. Obeng EA, Carlson LM, Gutman DM, et al. Proteasome inhibitors induce a terminal unfolded protein response in multiple myeloma cells. *Blood* 2006;107:4907–16.
29. Nawrocki ST, Carew JS, Pino MS, et al. Bortezomib sensitizes pancreatic cancer cells to endoplasmic reticulum stress-mediated apoptosis. *Cancer Res* 2005;65:11658–66.
30. Fribley A, Zeng Q, Wang C-Y. Proteasome inhibitor PS-341 induces apoptosis through induction of endoplasmic reticulum stress-reactive oxygen species in head and neck squamous cell carcinoma cells. *Mol Cell Biol* 2004;24:9695–704.
31. Chou T-C, Talalay P. Quantitative analysis of dose-effect relationships: the combined effects of multiple drugs or enzyme inhibitors. *Adv Enzyme Regul* 1984;22:27–55.
32. Kincaid MM, Cooper AA. ERADicate ER stress or die trying. *Antioxid Redox Signal* 2007;9:2373–87.
33. Novoa I, Zeng H, Harding HP, Ron D. Feedback inhibition of the unfolded protein response by GADD34-mediated dephosphorylation of eIF2 $\alpha$ . *J Cell Biol* 2001;153:1011–22.
34. Ma Y, Hendershot LM. Delineation of a negative feedback regulatory loop that controls protein translation during endoplasmic reticulum stress. *J Biol Chem* 2003;278:34864–73.
35. Harding HP, Novoa I, Zhang Y, et al. Regulated translation initiation controls stress-induced gene expression in mammalian cells. *Mol Cell* 2000;6:1099–108.
36. Lu PD, Harding HP, Ron D. Translation reinitiation at alternative open reading frames regulates gene expression in an integrated stress response. *J Cell Biol* 2004;167:27–33.
37. Guyton KZ, Xu Q, Holbrook NJ. Induction of the mammalian stress response gene GADD153 by oxidative stress: role of AP-1 element. *Biochem J* 1996;314:547–54.
38. Urano F, Wang X, Bertolotti A, et al. Coupling of stress in the ER to activation of JNK protein kinases by transmembrane protein kinase IRE1. *Science* 2000;287:664–6.
39. Shen Y, Ballar P, Apostolou A, Doong H, Fang S. ER stress differentially regulates the stabilities of ERAD ubiquitin ligases and their substrates. *Biochem Biophys Res Commun* 2007;352:919–24.
40. Sriburi R, Bommasamy H, Buldak GL, et al. Coordinate regulation of phospholipid biosynthesis and secretory pathway gene expression in XBP-1(S)-induced endoplasmic reticulum biogenesis. *J Biol Chem* 2007;282:7024–34.
41. Xu C, Bailly-Maitre B, Reed JC. Endoplasmic reticulum stress: cell life and death decisions. *J Clin Invest* 2005;115:2656–64.
42. Ma Y, Hendershot LM. The role of the unfolded protein response in tumour development: friend or foe? *Nat Rev Cancer* 2004;4:966–77.
43. Lin JH, Li H, Yasumura D, et al. IRE1 signaling affects cell fate during the unfolded protein response. *Science* 2007;318:944–9.
44. Novoa I, Zhang Y, Zeng H, et al. Stress-induced gene expression requires programmed recovery from translational repression. *EMBO J* 2003;22:1180–7.
45. Ron D, Walter P. Signal integration in the endoplasmic reticulum unfolded protein response. *Nat Rev Mol Cell Biol* 2007;8:519–29.
46. Calfon M, Zeng H, Urano F, et al. IRE1 couples endoplasmic reticulum load to secretory capacity by processing the XBP-1 mRNA. *Nature* 2002;415:92–6.
47. Lee A-H, Iwakoshi NN, Glimcher LH. XBP-1 regulates a subset of endoplasmic reticulum resident chaperone genes in the unfolded protein response. *Mol Cell Biol* 2003;23:7448–59.
48. Wang XZ, Harding HP, Zhang Y, et al. Cloning of mammalian Ire1 reveals diversity in the ER stress responses. *EMBO J* 1998;17:5708–17.
49. Zinszner H, Kuroda M, Wang X, et al. CHOP is implicated in programmed cell death in response to impaired function of the endoplasmic reticulum. *Genes Dev* 1998;12:982–95.

# Molecular Cancer Therapeutics

## Disruption of crosstalk between the fatty acid synthesis and proteasome pathways enhances unfolded protein response signaling and cell death

Joy L. Little, Frances B. Wheeler, Constantinos Koumenis, et al.

*Mol Cancer Ther* 2008;7:3816-3824.

<b>Updated version</b>	Access the most recent version of this article at: <a href="http://mct.aacrjournals.org/content/7/12/3816">http://mct.aacrjournals.org/content/7/12/3816</a>
<b>Supplementary Material</b>	Access the most recent supplemental material at: <a href="http://mct.aacrjournals.org/content/suppl/2008/12/08/7.12.3816.DC1">http://mct.aacrjournals.org/content/suppl/2008/12/08/7.12.3816.DC1</a>

<b>Cited articles</b>	This article cites 48 articles, 27 of which you can access for free at: <a href="http://mct.aacrjournals.org/content/7/12/3816.full#ref-list-1">http://mct.aacrjournals.org/content/7/12/3816.full#ref-list-1</a>
<b>Citing articles</b>	This article has been cited by 3 HighWire-hosted articles. Access the articles at: <a href="http://mct.aacrjournals.org/content/7/12/3816.full#related-urls">http://mct.aacrjournals.org/content/7/12/3816.full#related-urls</a>

<b>E-mail alerts</b>	<a href="#">Sign up to receive free email-alerts</a> related to this article or journal.
<b>Reprints and Subscriptions</b>	To order reprints of this article or to subscribe to the journal, contact the AACR Publications Department at <a href="mailto:pubs@aacr.org">pubs@aacr.org</a> .
<b>Permissions</b>	To request permission to re-use all or part of this article, use this link <a href="http://mct.aacrjournals.org/content/7/12/3816">http://mct.aacrjournals.org/content/7/12/3816</a> . Click on "Request Permissions" which will take you to the Copyright Clearance Center's (CCC) Rightslink site.